



HAL
open science

Diode-pumped mode-locked Yb:BaF₂ laser

Wen-Ze Xue, Zhang-Lang Lin, Huang-Jun Zeng, Ge Zhang, Pavel Loiko, Liza Basyrova, Abdelmjid Benayad, Patrice Camy, Valentin Petrov, Xavier Mateos, et al.

► **To cite this version:**

Wen-Ze Xue, Zhang-Lang Lin, Huang-Jun Zeng, Ge Zhang, Pavel Loiko, et al.. Diode-pumped mode-locked Yb:BaF₂ laser. Optics Express, 2022, 30 (9), pp.15807. 10.1364/OE.459704 . hal-03858729

HAL Id: hal-03858729

<https://hal.science/hal-03858729>

Submitted on 17 Nov 2022

HAL is a multi-disciplinary open access archive for the deposit and dissemination of scientific research documents, whether they are published or not. The documents may come from teaching and research institutions in France or abroad, or from public or private research centers.

L'archive ouverte pluridisciplinaire **HAL**, est destinée au dépôt et à la diffusion de documents scientifiques de niveau recherche, publiés ou non, émanant des établissements d'enseignement et de recherche français ou étrangers, des laboratoires publics ou privés.

To be published in Optics Express:

Title: Diode-pumped mode-locked Yb:BaF₂ laser

Authors: Wenze Xue,Zhanglang Lin,huangjun zeng,Zhang Ge,Pavel Loiko,liza Basyrova,Abdelmjid Benayad,Patrice Camy,Valentin Petrov,Xavier Mateos,Li Wang,Weidong Chen

Accepted: 13 April 22

Posted 18 April 22

DOI: <https://doi.org/10.1364/OE.459704>

© 2022 Optical Society of America under the terms of the [OSA Open Access Publishing Agreement](#)

OPTICA
PUBLISHING GROUP
Formerly OSA

Diode-pumped mode-locked Yb:BaF₂ laser

WEN-ZE XUE,¹ ZHANG-LANG LIN,¹ HUANG-JUN ZENG,¹ GE ZHANG,¹
PAVEL LOIKO,² LIZA BASYROVA,² ABDELMJID BENAYAD,² PATRICE CAMY,²
VALENTIN PETROV,³ XAVIER MATEOS,⁴ LI WANG³ AND WEIDONG CHEN^{1,3,*}

¹Fujian Institute of Research on the Structure of Matter, Chinese Academy of Sciences, 350002 Fuzhou, China

²Centre de Recherche sur les Ions, les Matériaux et la Photonique (CIMAP), UMR 6252 CEA-CNRS-ENSICAEN, Université de Caen, 6 Boulevard Maréchal Juin, 14050 Caen Cedex 4, France

³Max Born Institute for Nonlinear Optics and Short Pulse Spectroscopy, Max-Born-Str. 2a, 12489 Berlin, Germany

⁴Universitat Rovira i Virgili, URV, Física i Cristal·lografia de Materials i Nanomaterials (FiCMA-FiCNA)- Marcel·lí Domingo 1, 43007 Tarragona, Spain

*chenweidong@fjirsm.ac.cn

Abstract: We report on a continuous-wave (CW) and passively mode-locked operation of a fluorite-type Yb:BaF₂ crystal. Pumped with a spatially single-mode, fiber-coupled InGaAs laser diode at 976 nm, the Yb:BaF₂ laser generated a maximum CW output power of 512 mW at 1054.4 nm, corresponding to a laser threshold of 36.5 mW and a slope efficiency of 65.0%. A continuous wavelength tuning across 85 nm (1007 – 1092 nm) was achieved. By implementing a semiconductor saturable absorber mirror for initiating and sustaining the soliton pulse shaping, near Fourier-transform-limited pulses as short as 52 fs were generated at 1058.2 nm with an average output power of 129 mW at a pulse repetition rate of ~79.5 MHz. To the best of our knowledge, this is the first report on the passively mode-locked operation of the Yb:BaF₂ crystal.

© 2022 Optical Society of America under the terms of the [OSA Open Access Publishing Agreement](#)

1. Introduction

Alkaline-earth fluoride crystals with a chemical formula of MF₂, where M = Ca²⁺ [1, 2], Sr²⁺ [3] and Ba²⁺ [4] or their mixture [5], are attractive host materials for doping with trivalent rare-earth ions (RE³⁺) for laser applications. They belong to the cubic class exhibiting the so-called fluorite-type structure (fluorite is the mineral form of CaF₂), sp. gr. *Fm* $\bar{3}$ *m*. In RE³⁺-doped MF₂ crystals, the charge compensation is provided by interstitial F⁻ anions, M_{1-x}RE_xF_{2+x}. There exist several possibilities for incorporation of F⁻ ions, so that at low doping levels (<0.1 at.%), this leads to several non-equivalent sites for the dopant ions (trigonal, C_{3v}, tetragonal, C_{4v}, cubic, O_h). With increasing the doping level, the RE³⁺ ions in MF₂ crystals tend to form clusters [6, 7]. For >1 at.% doping, the majority of the ions form large clusters of different geometries. This results in profound inhomogeneous broadening of their absorption and emission bands (a “glassy-like” spectroscopic behavior).

Besides the broadband emission properties of the dopant RE³⁺ ions, the MF₂ crystals feature attractive physical properties as laser host matrices, in particular when compared to oxide crystals [8]. They exhibit broad transparency extending from the UV to the mid-IR, low refractive index, high thermal conductivity ($\kappa_0 = 9.7 \text{ Wm}^{-1}\text{K}^{-1}$ for undoped CaF₂) with a moderate dependence on the RE³⁺ doping level, negative thermo-optic coefficients leading to weak negative thermal lensing and low phonon energies. They can also be used in the form of ceramics [9].

So far, calcium fluoride (CaF₂) is the most widespread compound of the MF₂ crystal family. Concerning laser applications, in recent years, it has been mainly studied for doping with ytterbium (Yb³⁺) ions leading to broadband emission around 1 μm . A combination of the intrinsic features of the Yb³⁺ ion (simple energy-level scheme, low quantum defect under

48 resonant pumping), the smooth and broad (“*glassy-like*”) emission spectra of Yb^{3+} in CaF_2 , as
49 well as the advantageous thermo-mechanical properties of the host matrix determine the high
50 suitability of $\text{Yb}:\text{CaF}_2$ for the development of high-power diode-pumped femtosecond mode-
51 locked (ML) oscillators [10-13] and amplifiers [14-17]. Sévillano *et al.* reported on a Kerr-lens
52 mode-locked $\text{Yb}:\text{CaF}_2$ laser pumped by a high-brightness 979 nm fiber laser generating pulses
53 as short as 48 fs at 1046 nm corresponding to an average output power of 2.7 W at a repetition
54 rate of 73 MHz [18]. The longer fluorescence lifetime of $\text{Yb}:\text{CaF}_2$ ($^2\text{F}_{5/2}$, ~ 2.4 ms) ensures
55 efficient energy storage in Q-switched lasers and ultrafast amplifiers [19]. Siebold *et al.*
56 developed an $\text{Yb}:\text{CaF}_2$ -based chirped-pulse amplifier delivering femtosecond laser pulses at
57 1032 nm with a duration of 192 fs and a pulse energy of 197 mJ, which corresponded to a
58 terawatt-level peak power [20].

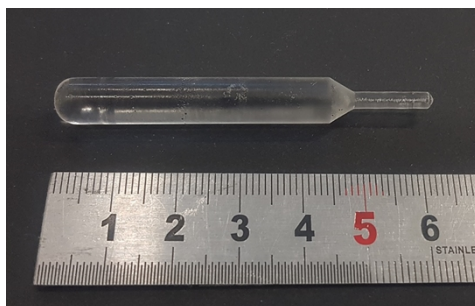
59 Barium fluoride (BaF_2) is another representative of the MF_2 family [21], being isostructural
60 to CaF_2 . It is commonly used for fabricating optical elements for the mid-IR part of the
61 spectrum, as well as fast scintillators. However, less attention has been paid to its applications
62 as a laser host matrix. It features even higher thermal conductivity ($\kappa_0 = 11.7 \text{ Wm}^{-1}\text{K}^{-1}$ for
63 undoped BaF_2) than its CaF_2 counterpart [4]. Camy *et al.* first reported on the continuous-wave
64 (CW) operation of the $\text{Yb}:\text{BaF}_2$ crystal: pumping with a Ti:Sapphire laser at 923 nm, the
65 maximum output power amounted to 100 mW at 1045 nm with a slope efficiency of 44% [4].
66 By using a Lyot filter, the spectral tuning range reached 55 nm (1006 – 1060 nm).

67 The promising spectroscopic and thermal properties of the $\text{Yb}:\text{BaF}_2$ crystal are attractive
68 for the development of sub-100 fs ML lasers. We are not aware of any reports on ultrashort
69 pulse generation using a $\text{Yb}:\text{BaF}_2$ crystal. In the present work, we report on the first passively
70 ML $\text{Yb}:\text{BaF}_2$ laser delivering soliton pulses as short as 52 fs. Our result also represents the
71 shortest pulse duration ever achieved from any *diode-pumped* ML $\text{Yb}:\text{MF}_2$ -based laser.

72 2. Experimental setup

73 2.1 Crystal growth

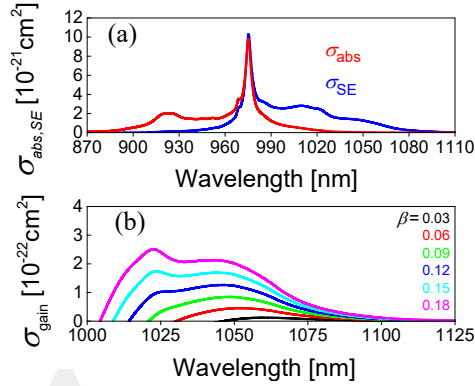
74 An $\text{Yb}:\text{BaF}_2$ crystal was grown by the Bridgman-Stockbarger technique with RF heating. As
75 starting reagents, we used BaF_2 and YbF_3 (purity: 4N). The initial Yb^{3+} doping level was 3 at.%
76 (with respect to Ba^{2+}). The powders were mixed and placed in a graphite crucible. A high
77 vacuum ($< 10^{-5}$ mbar) was created before introducing Ar and CF_4 gases to reduce oxygen
78 pollution. The growth was performed at $\sim 5^\circ\text{C}$ below the melting point of BaF_2 of about 1400°C .
79 The pulling rate was 1 – 3 mm/h. After the growth was completed, the crystal was slowly
80 cooled down to room temperature (20°C) within 48 h. The as-grown crystal was transparent,
81 colorless, and free of defects and inclusions, Fig. 1. The actual Yb^{3+} doping level (2.12 at.%,
82 $N_{\text{Yb}} = 3.56 \times 10^{20} \text{ cm}^{-3}$) was determined by Inductively Coupled Plasma Mass Spectrometry
83 (ICP-MS) leading to a segregation coefficient $K_{\text{Yb}} = 0.71$. The crystal was oriented using a Laue
84 diffractometer.



85
86 **Fig. 1.** A photograph of an as-grown $\text{Yb}:\text{BaF}_2$ crystal.

87 2.2 Optical spectroscopy

88 The absorption spectrum of Yb^{3+} in BaF_2 corresponding to the ${}^2\text{F}_{7/2} \rightarrow {}^2\text{F}_{5/2}$ transition is shown
 89 in Fig. 2(a). The maximum absorption cross-section σ_{abs} corresponding to the Yb^{3+} zero-
 90 phonon-line (ZPL) is $0.97 \times 10^{-20} \text{ cm}^2$ at 975.2 nm and the corresponding absorption bandwidth
 91 (full width at half maximum, FWHM) is 5.6 nm making this crystal promising for pumping
 92 with InGaAs laser diodes. The stimulated-emission (SE) cross-section, σ_{SE} , was calculated
 93 using a combination of the reciprocity method and the Fuchtbauer–Ladenburg formula,
 94 Fig. 2(a). In the spectral range where laser operation is expected (at wavelengths well above
 95 the ZPL), $\sigma_{\text{SE}} = 0.13 \times 10^{-20} \text{ cm}^2$ at 1049 nm.

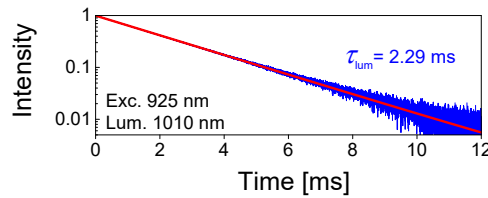


96
 97
 98
 99

Fig. 2. Spectroscopy of $\text{Yb}^{3+}:\text{BaF}_2$: (a) absorption, σ_{abs} , and stimulated-emission (SE), σ_{SE} , cross-sections; (b) gain cross-sections, $\sigma_{\text{gain}} = \beta\sigma_{\text{SE}} - (1 - \beta)\sigma_{\text{abs}}$, for different inversion ratios $\beta = N_2/N_{\text{Yb}}$.

100 According to the quasi-three-level nature of the Yb laser scheme with reabsorption, the gain
 101 cross-section, $\sigma_{\text{gain}} = \beta\sigma_{\text{SE}} - (1 - \beta)\sigma_{\text{abs}}$, of $\text{Yb}^{3+}:\text{BaF}_2$ was calculated as shown in Fig. 2(b).
 102 Here, $\beta = N_2/N_{\text{Yb}}$ is the inversion ratio and N_2 is the population of the upper laser level (${}^2\text{F}_{5/2}$).
 103 The gain spectra are smooth and broad (a “glassy-like” spectroscopic behavior). This is due to
 104 the strong inhomogeneous spectral broadening in all fluorite-type crystals (including BaF_2)
 105 originating from clustering of the Yb^{3+} dopant ions. With increasing the inversion ratio, the
 106 spectral maximum experiences a blue shift, from 1060 nm for small $\beta = 0.03$ to 1022 nm for
 107 high $\beta > 0.15$. The gain bandwidth (FWHM) for an intermediate $\beta = 0.12$ reaches 48 nm. This
 108 spectral behavior indicates the high potential of $\text{Yb}:\text{BaF}_2$ for broad wavelength tuning and
 109 sub-100 fs pulse generation from ML lasers.

110 The luminescence decay curve of Yb^{3+} ions in BaF_2 was measured using a finely powdered
 111 crystalline sample to avoid the effect of radiation trapping (reabsorption), Fig. 3. The Yb^{3+} ion
 112 luminescence exhibits a single-exponential decay with a characteristic lifetime $\tau_{\text{lum}} = 2.29 \text{ ms}$.



113
 114
 115

Fig. 3. The measured luminescence decay curve of the $\text{Yb}:\text{BaF}_2$ crystal, $\lambda_{\text{exc}} = 925 \text{ nm}$, $\lambda_{\text{lum}} = 1010 \text{ nm}$, red line – single-exponential fit.

116 Among other fluorite-type crystals, BaF_2 is known for its low phonon energy. The vibronic
 117 properties of the $\text{Yb}:\text{BaF}_2$ crystal were studied by Raman spectroscopy, Fig. 4. In the spectrum,
 118 a single intense peak appears centered at 242 cm^{-1} with a (FWHM) of 12 cm^{-1} . BaF_2 has a
 119 triatomic unit-cell and, therefore, it has only one first-order Raman-active mode of type F_{2g}
 120 [22]. No defect-related peaks are observed in the spectrum.

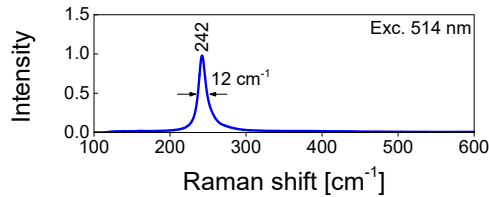


Fig. 4. Unpolarized Raman spectrum of the Yb:BaF₂ crystal, $\lambda_{\text{exc}} = 514$ nm.

2.3 Laser set-up

For the laser experiments, we prepared a cubic sample cut from the as-grown Yb:BaF₂ crystal with an aperture of 3 mm × 3 mm and a thickness of 3 mm oriented along the [111] axis. It was polished to laser-grade quality from both sides and remained uncoated. The scheme of the Yb:BaF₂ laser is shown in Fig. 5. The laser crystal was mounted on a copper holder without active cooling and placed in an astigmatically compensated X-shaped standing-wave cavity between the two concave folding mirrors M₁ and M₂ (radius of curvature, RoC = -100 mm) with the Brewster minimum loss condition fulfilled for the laser wavelength. A spatial-single-mode, fiber-coupled InGaAs laser diode delivering a maximum incident power of 1.29 W (unpolarized radiation) was used as a pump source. Its emission wavelength was locked at 976 nm with a spectral linewidth (FWHM) of ~0.2 nm by using a fiber Bragg grating (FBG). The measured beam propagation factor (M²) of the pump radiation at the maximum output power was ~1.02. The pump beam was collimated and focused into the laser crystal by using an aspherical lens L₁ (focal length: $f = 26$ mm) and an achromatic doublet lens L₂ ($f = 100$ mm) yielding a beam waist (radius) of 18.7 $\mu\text{m} \times 33.5 \mu\text{m}$ in the sagittal and tangential planes, respectively.

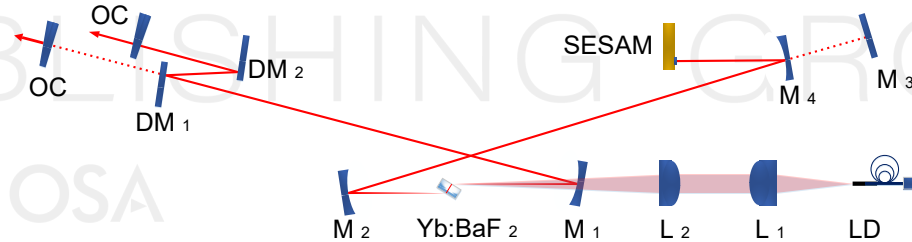


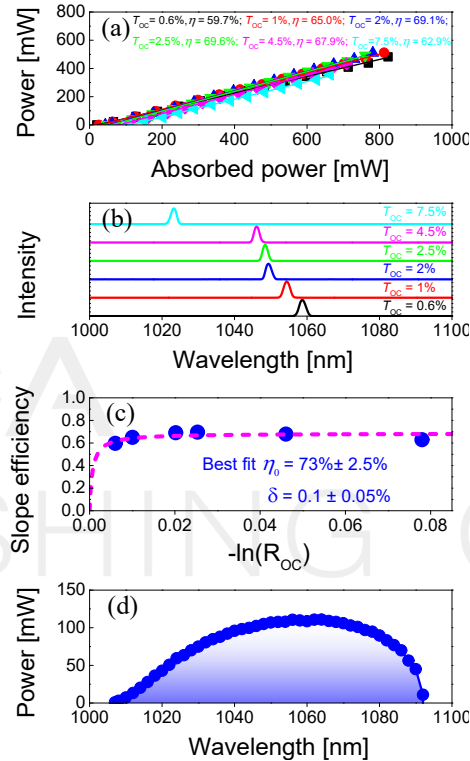
Fig. 5. Experimental configuration of the Yb:BaF₂ laser. LD: fiber-coupled InGaAs laser diode; L₁: aspherical lens; L₂: achromatic doublet lens; M₁, M₂ and M₄: curved mirrors (RoC = -100 mm); M₃: flat rear mirror for CW laser operation; DM₁ and DM₂: flat dispersive mirrors; OC: output coupler; SESAM: SEMiconductor Saturable Absorber Mirror.

A four-mirror cavity was used in the CW regime. One cavity arm was terminated by a flat rear mirror M₃ and the other arm – by a plane-wedged output coupler (OC) with a transmission at the laser wavelength T_{OC} in the 0.6% - 7.5% range. The radius of the fundamental laser mode in the Yb:BaF₂ crystal estimated using the ABCD method was 22.7 $\mu\text{m} \times 33.0 \mu\text{m}$ in the sagittal and the tangential planes, respectively. The measured single-pass pump absorption under lasing conditions depended on the transmission of the OC ranging from 76.7% to 81%.

For ML operation, the flat rear mirror M₃ was substituted by a curved mirror M₄ (RoC = -100 mm) for creating a second beam waist on the SESAM with a calculated beam radius of ~52 μm to ensure its efficient bleaching. Two commercial SESAMs (BATOP, GmbH) were implemented. Two flat dispersive mirrors (DM₁ and DM₂) with a negative group delay dispersion (GDD) per bounce of -250 fs² were introduced in the other cavity arm to compensate the material dispersion of the BaF₂ crystal (26.6 fs²/mm at 1050 nm) and to balance the self-phase modulation (SPM) for soliton pulse shaping. The geometrical cavity length of the ML laser was 1.88 m, corresponding to a pulse repetition rate of ~79.6 MHz.

3. Continuous-wave laser operation

159 In the CW regime, the BaF₂ laser generated a maximum output power of 512 mW at 1054.4 nm
 160 for an absorbed pump power of 0.813 W with a laser threshold of 36.5 mW, which
 161 corresponded to a slope efficiency of 65.0% for $T_{OC} = 1\%$, see Fig. 6(a). Slightly higher slope
 162 efficiency of 69.6% was achieved with $T_{OC} = 2.5\%$ corresponding to an output power of
 163 493 mW at an absorbed power of 0.761 W. The laser threshold gradually increased with the
 164 output coupling, from 26.9 mW ($T_{OC} = 0.6\%$) to 190.9 mW ($T_{OC} = 7.5\%$). The laser wavelength
 165 experienced a monotonic blue-shift with increasing T_{OC} in the range of 1023.2 – 1058.7 nm, as
 166 shown in Fig. 6(b). This behavior is typical for quasi-three-level Yb lasers with inherent
 167 reabsorption at the laser wavelength.



168 **Fig. 6.** CW diode-pumped Yb:BaF₂ laser: (a) input - output dependences for different OCs,
 169 η – slope efficiency; (b) typical spectra of laser emission; (c) Caird analysis: slope efficiency vs.
 170 $R_{OC} = 1 - T_{OC}$; (d) tuning curve obtained with a Lyot filter and $T_{OC} = 0.4\%$.
 171

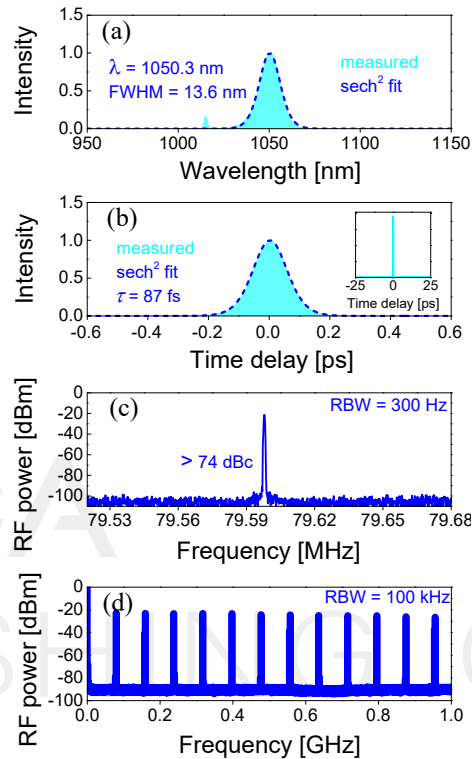
172 The Caird analysis was applied by fitting the measured laser slope efficiency as a function
 173 of the output coupler reflectivity, $R_{OC} = 1 - T_{OC}$ [23]. The total round-trip cavity losses δ
 174 (reabsorption losses excluded), as well as the intrinsic slope efficiency η_0 (accounting for the
 175 mode-matching and the quantum efficiencies) were estimated yielding $\eta_0 = 73 \pm 2.5\%$ and
 176 $\delta = 0.1 \pm 0.05\%$, as shown in Fig. 6(c). The low value of δ evidences the good optical quality
 177 of the laser crystal.

178 The wavelength tuning of the Yb:BaF₂ laser in the CW regime was studied by inserting a
 179 Lyot filter close to the OC ($T_{OC} = 0.4\%$) at an incident pump power of 400 mW. The laser
 180 wavelength was continuously tunable between 1007 and 1092 nm, i.e., across 85 nm at the
 181 zero-level, Fig. 6(d).

182 4. Mode-locked laser operation

183 Initially, a SESAM with a modulation depth of 1.2% and a relaxation time of ~ 1 ps was
 184 implemented to start and stabilize the ML operation of the Yb:BaF₂ laser. A total round-trip

185 negative GDD of -1000 fs^2 was introduced by using two flat DMs ($\text{DM}_1 - \text{DM}_2$), see Fig. 5.
 186 After careful cavity alignment, stable and self-starting ML operation was readily achieved with
 187 a 4% OC. The measured optical spectrum of the laser pulses had an emission bandwidth of
 188 13.6 nm by assuming a sech^2 -shaped intensity profile at a central wavelength of 1050.3 nm, see
 189 Fig. 7(a).

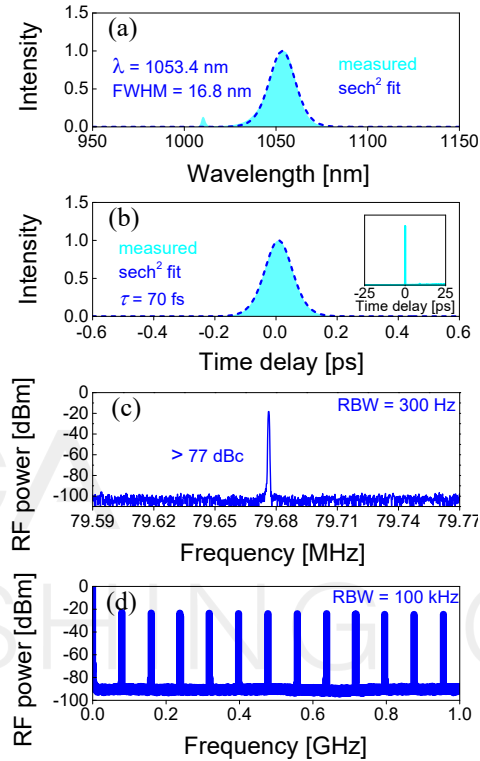


190
 191 **Fig. 7.** SESAM ML Yb:BaF₂ laser with $T_{\text{OC}} = 4\%$. (a) Optical spectrum and (b) SHG-based
 192 intensity autocorrelation trace. *Inset:* autocorrelation trace on a time span of 50 ps. (c) First beat
 193 note at ~ 79.59 MHz of the RF spectrum recorded with a resolution bandwidth (RBW) of 300 Hz,
 194 and (d) RF harmonics on a 1-GHz frequency span recorded with an RBW of 100 kHz.

195 The recorded intensity autocorrelation trace was almost perfectly fitted with a sech^2 -shaped
 196 temporal pulse profile giving a pulse duration (FWHM) of 87 fs corresponding to a time-
 197 bandwidth-product (TBP) of 0.322, see Fig. 7(b). An average output power of 270 mW was
 198 obtained at an absorbed pump power of 618 mW, corresponding to an optical efficiency of
 199 43.6% and a peak power of 34.1 kW. The inset of Fig. 7(b) shows the measured intensity
 200 autocorrelation trace on a long-time span of 50 ps indicating single-pulse CW-ML operation
 201 free of multiple pulse instabilities. A radio-frequency (RF) spectrum analyzer was used for
 202 evaluating the stability of the ML operation. The relatively high extinction ratio of >74 dBc
 203 above the noise level for the first beat note at 79.59 MHz in combination with the uniform
 204 harmonics recorded on a 1-GHz frequency span are evidence for highly stable ML operation
 205 without any unwanted Q-switching or multi-pulsing instabilities, see Fig. 7(c) and (d).

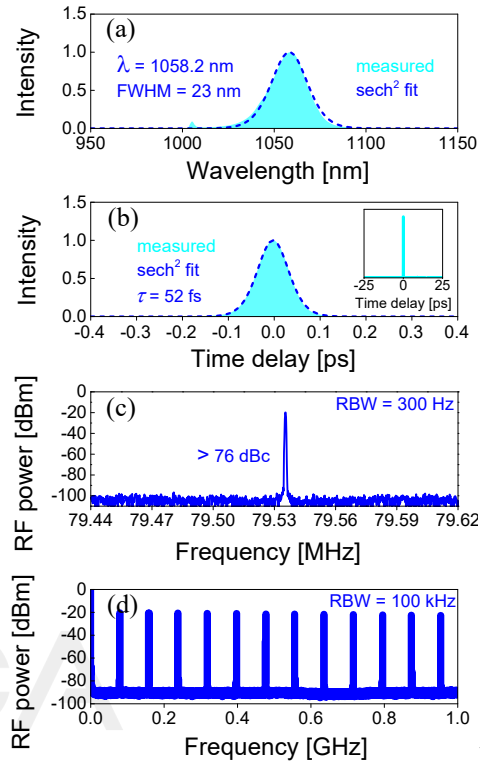
206 Shorter pulses could be achieved by using a SESAM with higher modulation depth of 3%.
 207 With a 2.5% OC, the Yb:BaF₂ laser delivered pulses with a spectral bandwidth of 16.8 nm at a
 208 central wavelength of 1053.4 nm by assuming a sech^2 -shaped intensity profile, see Fig. 8(a).
 209 The almost perfect fit of the recorded intensity autocorrelation trace using a sech^2 -shaped
 210 temporal intensity profile resulted in an estimated pulse duration of 70 fs, see Fig. 8(b). The
 211 50-ps long-time scale autocorrelation trace revealed single-pulse mode-locking, see the inset of
 212 Fig. 8(b). The corresponding TBP amounted to 0.318 which was very close to the Fourier-

213 transform-limited value of 0.315. The average output power amounted to 168 mW at an
 214 absorbed pump power of 531 mW, corresponding to an optical efficiency of 31.6% and a peak
 215 power of 26.4 kW. The measured RF spectra are shown in Fig. 8(c) and (d). Recorded at a
 216 resolution bandwidth of 300 Hz on a ~180 kHz span, the first beat note at 79.67 MHz displays
 217 an extinction ratio of >77 dBc above carrier. A 1-GHz wide-span RF measurement with an
 218 RBW of 100 kHz provided further evidence of stable single-pulse CW-ML operation.



219
 220 **Fig. 8.** SESAM ML Yb:BaF₂ laser with $T_{OC} = 2.5\%$. (a) Optical spectrum and (b) SHG-based
 221 intensity autocorrelation trace. *Inset:* autocorrelation trace on a time span of 50 ps. (c, d) RF
 222 spectra: (c) First beat note at ~79.67 MHz recorded with an RBW of 300 Hz, and (d) Harmonics
 223 on a 1-GHz frequency span recorded with an RBW of 100 kHz.

224 The shortest pulses with ultimate stability were achieved with the same SESAM using a 2%
 225 OC. Assuming a sech^2 -shaped spectral intensity profile, an emission bandwidth of 23 nm was
 226 obtained at a central wavelength of 1058.2 nm, see Fig. 9(a). Figure 9(b) shows the recorded
 227 intensity autocorrelation trace for the shortest pulses. The curve can be almost perfectly fitted
 228 with a sech^2 -shape temporal profile, yielding an estimate of 52 fs for the pulse duration. This
 229 corresponds to a TBP of 0.320 which is only slightly above the Fourier-transform-limit. A
 230 longer time-scale intensity autocorrelation trace recorded within a 50-ps time range indicated
 231 single-pulse CW-ML operation without multi-pulsing instabilities, see inset of the Fig. 9(b).
 232 The average output power amounted to 129 mW at an absorbed pump power of 578 mW, which
 233 corresponded to an optical efficiency of 22.3% and a peak power of 27.3 kW. The RF spectra
 234 of the shortest pulses were recorded to verify the stability of the ML operation in different
 235 frequency span ranges, as shown in Fig. 9(c) and (d). The recorded fundamental beat note
 236 located at 79.54 MHz exhibited a high extinction ratio of >76 dBc above carrier. The measured
 237 uniform harmonics on a 1-GHz frequency span again revealed high stability of the single-pulse
 238 ML operation.



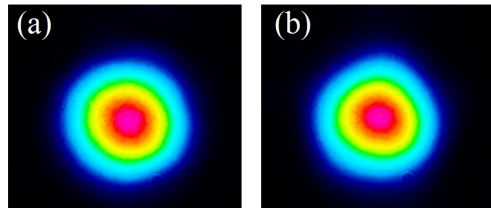
239

240
241
242
243

Fig. 9. SESAM ML Yb:BaF₂ laser with $T_{oc} = 2\%$. (a) Optical spectrum and (b) SHG-based intensity autocorrelation trace. *Inset:* autocorrelation trace on a time span of 50 ps. (c, d) RF spectra: (c) Fundamental beat note at 79.54 MHz recorded with an RBW of 300 Hz, and (d) Harmonics on a 1-GHz frequency span recorded with an RBW of 100 kHz.

244
245
246
247
248
249
250
251
252
253

In order to confirm the pulse shaping mechanism, far-field beam profiles of the Yb:BaF₂ laser both in the CW and ML regimes were recorded with a IR camera placed at ~ 1.2 m from the OC. It was relatively easy to switch between the ML and CW laser operation regimes by a slight cavity misalignment. Almost unchanged beam diameters in the far-field were observed during such switching, see Fig. 10. The absent variation in the far-field beam profiles in combination with the nearly perfect sech²-shaped spectral and temporal profiles of the shortest pulses indicate that soliton mode-locking was the dominant pulse shaping mechanism rather than the Kerr-lens mode-locking. This conclusion is in line with the small value of the nonlinear refractive index n_2 of BaF₂ at ~ 1 μm (1.4×10^{-20} m²/W – 2.85×10^{-20} m²/W [24]), resulting in a relatively low nonlinear amplitude modulation with the 3 mm-thick crystal.



254
255

Fig. 10. Measured far-field beam profiles of the Yb:BaF₂ laser: (a) CW and (b) ML operation.

256

5. Conclusion

257
258

To conclude, ytterbium-doped barium fluoride (Yb:BaF₂) is a promising crystal for broadly tunable lasers and especially power-scalable ultrafast (sub-100 fs) oscillators emitting around

259 1 μm . It provides broad and intense absorption at the Yb^{3+} zero-phonon line facilitating its diode
260 pumping, broad (~ 50 nm) and smooth gain spectra extending until 1125 nm, as well as long
261 luminescence lifetime (2.29 ms). In the present work, we report on the first diode-pumped
262 continuous-wave and passively mode-locked $\text{Yb}:\text{BaF}_2$ lasers. By using a high-brightness pump
263 source (a cost-effective single-mode fiber-coupled InGaAs laser diode), a commercial SESAM
264 for initiating and sustaining the mode-locked operation and a pair chirped mirrors for
265 intracavity GDD dispersion management, soliton pulses as short as 52 fs were generated at a
266 central wavelength of 1058.2 nm corresponding to an average output power of 129 mW at a
267 pulse repetition rate of ~ 79.5 MHz. Our laser results indicate the potential of $\text{Yb}:\text{BaF}_2$ crystals
268 with optimized Yb^{3+} ion doping levels and thickness for further power scaling and pulse
269 shortening via the Kerr-lens mode-locking technique.

270 **Funding.** National Key Research and Development Program of China (2021YFB3601504); National Natural Science
271 Foundation of China (61975208, 61905247, 61875199, U21A20508, 61850410533); Sino-German Scientist
272 Cooperation and Exchanges Mobility Program (M-0040), Grant PID2019-108543RB-I00 funded by MCIN/AEI/
273 10.13039/501100011033.

274 **Acknowledgment.** Xavier Mateos acknowledges the Serra Hünter program.

275 **Disclosures.** The authors declare no conflicts of interest.

276 **Data availability.** Data underlying the results presented in this paper are not publicly available at this time but may
277 be obtained from the authors upon reasonable request.

278 References

- 279 1. M. Siebold, S. Bock, U. Schramm, B. Xu, J. L. Doualan, P. Camy and R. Moncorge, "Yb:CaF₂ - a new old laser
280 crystal," *Appl. Phys. B* **97**(2), 327-338 (2009).
- 281 2. V. Petit, J. L. Doualan, P. Camy, V. Ménard and R. Moncorgé, "CW and tunable laser operation of Yb³⁺ doped
282 CaF₂," *Appl. Phys. B* **78**(6), 681-684 (2004).
- 283 3. M. Siebold, J. Hein, M. C. Kaluza and R. Uecker, "High-peak-power tunable laser operation of Yb:SrF₂," *Opt.*
284 *Lett.* **32**(13), 1818-1820 (2007).
- 285 4. P. Camy, J. L. Doualan, A. Benayad, M. Von Edlinger, V. Ménard and R. Moncorgé, "Comparative
286 spectroscopic and laser properties of Yb³⁺-doped CaF₂, SrF₂ and BaF₂ single crystals," *Appl. Phys. B* **89**(4),
287 539-542 (2007).
- 288 5. J. L. Doualan, P. Camy, A. Benayad, V. Ménard, R. Moncorgé, J. Boudeile, F. Druon, F. Balembois, and P.
289 Georges, "Yb³⁺ doped (Ca, Sr, Ba)F₂ for high power laser applications," *Laser Phys.* **20**(2), 533-536 (2010).
- 290 6. V. Petit, P. Camy, J.-L. Doualan, X. Portier, and R. Moncorgé, "Spectroscopy of Yb³⁺:CaF₂: from isolated
291 centers to clusters," *Phys. Rev. B* **78**(8), 085131-1-12 (2008).
- 292 7. B. Lacroix, C. Genevois, J. L. Doualan, G. Brasse, A. Braud, P. Ruterana, P. Camy, E. Talbot, R. Moncorgé,
293 and J. Margerie, "Direct imaging of rare-earth ion clusters in Yb:CaF₂," *Phys. Rev. B* **90**(12), 125124-1-14
294 (2014).
- 295 8. F. Druon, S. Ricaud, D. N. Papadopoulos, A. Pellegrina, P. Camy, J. L. Doualan, R. Moncorgé, A. Courjaud, E.
296 Mottay and P. Georges, "On Yb:CaF₂ and Yb:SrF₂: review of spectroscopic and thermal properties and their
297 impact on femtosecond and high power laser performance," *Opt. Mater. Express* **1**(3), 489-502 (2011).
- 298 9. P. Aballea, A. Saganuma, F. Druon, J. Hostalrich, P. Georges, P. Gredin and M. Mortier, "Laser performance of
299 diode-pumped Yb:CaF₂ optical ceramics synthesized using an energy-efficient process," *Optica* **2**(4), 288-291
300 (2015).
- 301 10. F. Friebe, F. Druon, J. Boudeile, D. N. Papadopoulos, M. Hanna, P. Georges, P. Camy, J. L. Doualan, A.
302 Benayad, R. Moncorge, C. Cassagne and G. Boudebs, "Diode-pumped 99 fs Yb:CaF₂ oscillator," *Opt. Lett.*
303 **34**(9), 1474-1476 (2009).
- 304 11. G. Machinet, P. Sevilano, F. Guichard, R. Dubrasquet, P. Camy, J. L. Doualan, R. Moncorgé, P. Georges, F.
305 Druon, D. Descamps and E. Cormier, "High-brightness fiber laser-pumped 68 fs-2.3 W Kerr-lens mode-locked
306 Yb:CaF₂ oscillator," *Opt. Lett.* **38**(9), 4008-4010 (2013).
- 307 12. F. Druon, D. N. Papadopoulos, J. Boudeile, M. Hanna, P. Georges, A. Benayad, P. Camy, J. L. Doualan, V.
308 Menard and R. Moncorge, "Mode-locked operation of a diode-pumped femtosecond Yb:SrF₂ laser," *Opt. Lett.*
309 **34**(15), 2354-2356 (2009).
- 310 13. A. Lucca, G. Debourg, M. Jacquemet, F. Druon, F. Balembois, P. Georges, P. Camy, J. L. Doualan and R.
311 Moncorge, "High-power diode-pumped Yb³⁺:CaF₂ femtosecond laser," *Opt. Lett.* **29**(23), 2767-2769 (2004).
- 312 14. G. Machinet, G. Andriukaitis, P. Sévillano, J. Lhermite, D. Descamps, A. Pugžlys, A. Baltuška and E. Cormier,
313 "High-gain amplification in Yb:CaF₂ crystals pumped by a high-brightness Yb-doped 976 nm fiber laser,"
314 *Appl. Phys. B* **111**(3), 495-500 (2013).

- 315
316
317
318
319
320
321
322
323
324
325
326
327
328
329
330
331
332
333
334
335
336
337
338
15. D. N. Papadopoulos, F. Friebel, A. Pellegrina, M. Hanna, P. Camy, J. L. Doualan, R. Moncorge, P. Georges and F. P. H. J. Druon, "High repetition rate Yb:CaF₂ multipass amplifiers operating in the 100-mJ range," *IEEE J. Sel. Top. Quantum Electron.* **21**(1), 3100211 (2015).
 16. F. Druon, K. Genevri er, P. Georges and D. N. Papadopoulos, "Comparison of multi-pass and regenerative strategies for energetic high-gain amplifiers based on Yb:CaF₂," *Opt. Lett.* **45**(16), 4408-4411 (2020).
 17. S. Ricaud, P. Georges, P. Camy, J. L. Doualan, R. Moncorge, A. Courjaud, E. Mottay and F. Druon, "Diode-pumped regenerative Yb:SrF₂ amplifier," *Appl. Phys. B* **106**(4), 823-827 (2012).
 18. P. Sevillano, G. Machinet, R. Dubrasquet, P. Camy, J. L. Doualan, R. Moncorge, P. Georges, F. P. Druon, D. Descamps, E. E. D. H. G. Cormier and P. Moulton, "Sub-50 fs, Kerr-lens mode-locked Yb:CaF₂ laser oscillator delivering up to 2.7 W," in *Advanced Solid-State Lasers Congress* (Optical Society of America, Paris), p. AF3A.6 (2013).
 19. S. Ricaud, F. Druon, D. N. Papadopoulos, P. Camy, J. L. Doualan, R. Moncorge, M. Delaigue, Y. Zaouter, A. Courjaud, P. Georges and E. Mottay, "Short-pulse and high-repetition-rate diode-pumped Yb:CaF₂ regenerative amplifier," *Opt. Lett.* **35**(14), 2415-2417 (2010).
 20. M. Siebold, M. Hornung, R. Boedefeld, S. Podleska, S. Klingebiel, C. Wandt, F. Krausz, S. Karsch, R. Uecker, A. Jochmann, J. Hein and M. C. Kaluza, "Terawatt diode-pumped Yb:CaF₂ laser," *Opt. Lett.* **33**(23), 2770-2772 (2008).
 21. I. H. Malitson, "Refractive properties of barium fluoride," *J. Opt. Soc. Am.* **54**(5), 628-632 (1964).
 22. A. R. Gee, D. C. O'Shea, and H. Z. Cummins, "Raman scattering and fluorescence in calcium fluoride," *Solid-State Commun.* **4**(1), 43-46 (1966).
 23. J. A. Caird, S. A. Payne, P. Staber, A. Ramponi, L. Chase, and W. F. Krupke, "Quantum electronic-properties of the Na₃Ga₂Li₃F₁₂:Cr³⁺ laser," *IEEE J. Quantum Electron.* **24**(6), 1077 - 1099 (1988).
 24. T. R. Ensley and N. K. Bambha, "Ultrafast nonlinear refraction measurements of infrared transmitting materials in the mid-wave infrared," *Opt. Express* **27**(26), 37940-37951 (2019).

OPTICA
PUBLISHING GROUP

Formerly OSA